

Design of a 4-pole Line Start Permanent Magnet Synchronous Motor

F. Libert¹, J. Soulard¹ and J. Engström²

¹ Royal Institute of Technology
Department of Electrical Machines and Power Electronics,
100 44 Stockholm, Sweden
e-mail: florence@ekc.kth.se
e-mail: juliette@ekc.kth.se

² ITT Flygt AB
Box 1309, 171 25 Solna, Sweden
e-mail: jorgen.engstrom@flygt.com

Abstract— To improve the efficiency of submersible pumps, the solution described in this article consists in replacing the rotor of the induction motor with a rotor presenting a squirrel cage and buried permanent magnets that can start on the grid. The analytical procedure to design the rotor is presented with magnets placed in U shape and a four-pole motor. The steady state and transient performances of the different designed motors are then studied using finite element calculations and analytical models. As an example, the design of a 75kW four-pole motor is described.

List of principal symbols

List of used symbols:

B	Flux density
E_0	Induced voltage at synchronous speed
g	Air-gap length
i_{dr}	Rotor d-current
i_{qr}	Rotor q-current
i_{ds}, I_d	Stator d-current
i_{qs}, I_q	Stator q-current
L	Inductance
R_s	Stator resistance
R_{rpu}	Rotor bar resistance in per unit
T	Synchronous torque
u	Voltage
ω_s	Synchronous electrical speed
x_{ds}, X_d	Stator reactance in the d-axis
x_{qs}, X_q	Stator reactance in the q-axis
ψ	Flux linkage

List of subscript:

dr	Rotor d-axis
ds	Stator d-axis
m	Magnet
md	Mutual d-axis
mq	Mutual q-axis
qr	Rotor q-direction
qs	Stator q-direction
r	Rotor
s	Stator

1. Introduction

In order to decrease gas emissions, different countries led by the United States imposed classes of efficiency for stand-alone induction motors through their legislation.

Even though it is possible to increase the efficiency of traditional induction motors, this cannot be easily done without oversizing the motor, which is definitely contrary to the idea of an integrated motor for products such as pumps. In this case, the solution could be to find another type of motor that reaches higher efficiency levels: the Line Start Permanent Magnet Synchronous Motor (LSPM) is one of them. By introducing permanent magnets buried beneath the squirrel cage, a hybrid rotor is obtained which combines an asynchronous start with a synchronous steady state operation. With really low copper losses at steady state (harmonics losses only), a better efficiency can be reached.

The design procedure, which will be described in this paper, has been used on a 75kW four-pole motor. Different designs were tested in order to find a good compromise between good steady state performances and a good start and synchronization.

2. Design procedure

A: Start and synchronization of the LSPMs

The design of this kind of hybrid rotors is tricky. If the performances in steady state define the required volume of magnet, it is the transients that imposes the size of the squirrel cage. At start, a braking torque from the magnets is added to the load torque [1]. Figure 1 shows the different torques as a function of the speed during the transients.

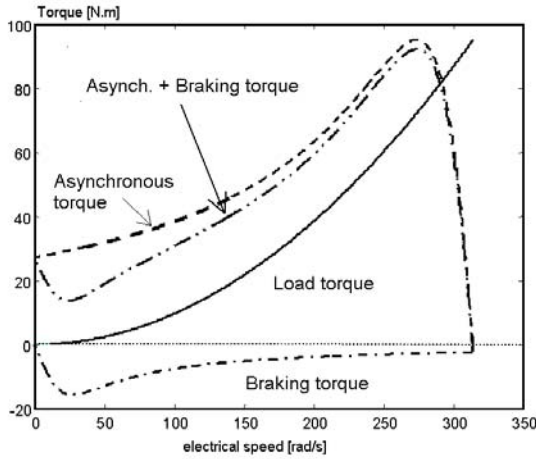


Fig. 1. Example of the evolution of different torques during the transients

The expression of the magnet braking torque as a function of the equivalent electrical parameters of the LSPM is:

$$T_b = \frac{3pR_s(1-s)^2 E_0^2}{2\omega_s(1-s)} \cdot \frac{R_s^2 + X_{qs}^2(1-s)^2}{(R_s^2 + X_{qs}X_{ds}(1-s))^2} \quad (1)$$

This torque is proportional to the square of the no-load voltage. If the volume of magnet in the rotor is too high then some problems at start can occur (see paragraph 2).

Therefore a compromise has to be found in order to combine a good start and synchronization, and good steady state performances. Taking into account these considerations, an analytical design procedure has been developed [2] and improved for the design of a 75kW four-pole motor.

B. The design procedure

For economical reasons, the stator and windings of the LSPM are identical to the induction motor of the same power used at present in the pumps. This means that between the induction motor and the LSPM, only the rotor is changed. The flow chart in figure 2 shows the important steps in the design procedure.

1) *Analytical calculation of the geometry* At first the data concerning the power and the stator of the motor are entered. The user chooses the configuration of the magnets: for each pole either 3 magnets placed in U or two magnets placed in V under the squirrel cage.

The squirrel cage is then designed giving the value of the rotor cage resistance, the level of saturation in a rotor tooth and the number of bars (chosen according to the number of stator slots to minimize the oscillations at start).

The exterior magnets are placed directly under one bar to heavily saturate the iron bridges and allow the magnetization of the air-gap. For a low harmonic content, an electrical pole angle near to 120° has been chosen. The magnets have all the same dimensions because of economical reasons. The magnet dimensions are calculated analytically in order to obtain the chosen no-load voltage [3].

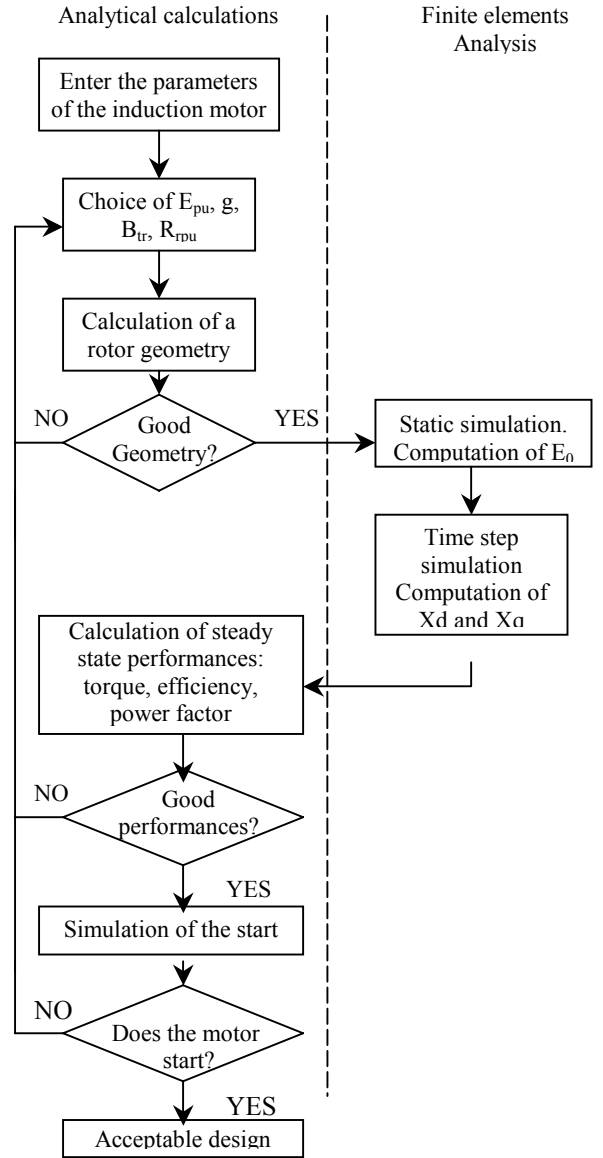


Fig. 2. Flow chart summarizing the design procedure

This analytical design procedure has been implemented in Matlab. As the whole program is analytical, its execution takes only few seconds. The geometry of the rotor can be plotted. This allows studying the influence of the parameters chosen by the user, the possibility to manufacture the obtained rotor and having a first check of the magnets volume that is required. Figure 3 presents the geometry of a 4 poles LSPM with magnets placed in U.

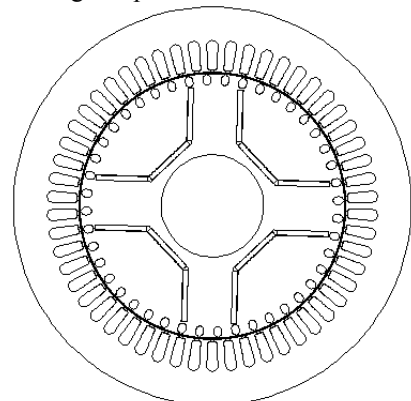


Fig. 3. Geometry of a 4 poles LSPM with U-shape magnets

2) *Finite element simulation* The finite element simulations allow at first to confirm the analytical results for the no-load voltage. The direct and quadrature reactances that are needed to compute the performances can then be obtained. The analytical calculation of the inductances is not accurate enough because it is difficult to define an analytical model of the saturation between the magnets and the bars.

Different methods can be used to analyse the simulations, depending on the size of the finite element problem. Time-step FEM simulations with fixed speed can now be conducted in a relative short time depending on the size of the problem (reduced geometry thanks to symmetries). In the case of the 75kW 4 pole LSPM, half the motor needed to be simulated because of the complex double layer winding. Adapted methods were used to avoid time-consuming simulations.

With a static simulation the flux density in the air-gap (figure 4) and the no-load voltage can be plotted and compared to the expected analytical values. For the 75kW LSPM, the no-load voltage is retrieved from the magnetic vector potentials obtained in the same static simulation [4].

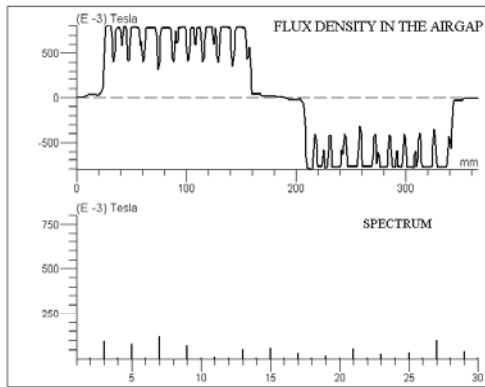


Fig. 4. Flux density in the air-gap for a test-geometry

To compute the d- and q- axis reactances X_d and X_q in the case of the 75kW LSPM, a time-step simulation is run. The rotor keeps the same position while the stator slots are fed with sinusoidal currents. The currents are chosen so that the ratio I_d/I_q is constant. When analysing the results of the simulation, the d- and q- axis linkage Ψ_d and Ψ_q are computed from the flux seen by each phase winding with a Park transformation. The reactances are then found as a function of I_d and I_q using:

$$X_d = 2\pi f \frac{\Psi_d - \Psi_m}{I_d} \quad (2)$$

$$X_q = 2\pi f \frac{\Psi_q}{I_q} \quad (3)$$

where Ψ_m is the flux created by the magnets. This way, one can get as well the influence of the current amplitude on the reactances. Figure 5 represents the curves of X_d and X_q as a function of I_d and I_q for the third design present in paragraph 3 of this paper.

3) *Performances* The next step is to check whether the designed motor fulfils the required performances or not. The steady state performances, efficiency, power

factor, synchronous torque are computed analytically and compared to the induction motor's performances. The start and synchronization are then simulated. If the motor does not synchronize, the design procedure has to be run again. The way to simulate the start and synchronization is described in the next part of the paper.

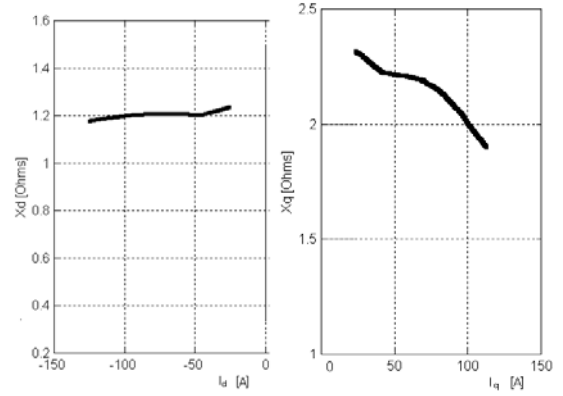


Fig. 5. d- and q axis reactances calculated with finite element simulations as a function of I_d and I_q .

2. Problems at start

A LSPM, which presents good steady state performances, may have some problems to start and synchronize. The start can fail because of a too high magnet braking torque in comparison to the asynchronous torque (see case 1 on figure 6). Problems can also be due to a high inertia or a too high rotor resistance combining with too thin magnets [5] (Case 2 on figure 6). The figure 6 presents the plot of the speed as a function of time for the three cases at start. In order to simulate the start of the motor, an analytical dq model has been implemented in Matlab. Finite element time step simulations can also be conducted but are much more time-consuming [6,7].

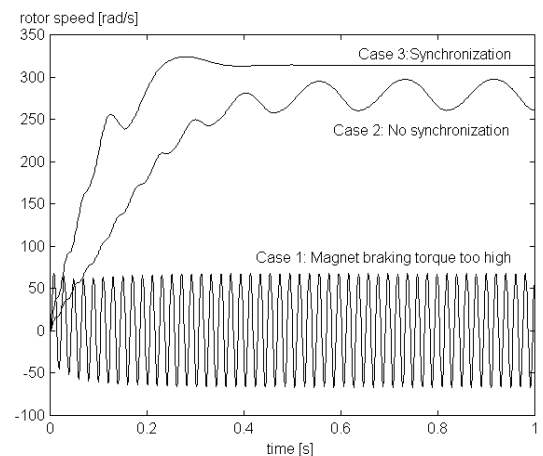


Fig. 6. Possible behaviour of LSPM at start

A. Machine model in the d-q system

The complete transformed machine model can be expressed as:

$$\begin{cases} u_{ds} = R_s i_{ds} + \frac{d\Psi_{ds}}{dt} - (1-s)\omega_s \Psi_{qs} \\ u_{qs} = R_s i_{qs} + \frac{d\Psi_{qs}}{dt} - (1-s)\omega_s \Psi_{ds} \end{cases} \quad (4)$$

where s is the slip defined as

$$s = \frac{n_s - n_r}{n_s} \quad (5)$$

where n_s and n_r are respectively the synchronous and rotor speeds.

$$\begin{cases} u_{dr} = R_{dr} i_{dr} + \frac{d\Psi_{dr}}{dt} = 0 \\ u_{qr} = R_{qr} i_{qr} + \frac{d\Psi_{qr}}{dt} = 0 \end{cases} \quad (6)$$

$$\begin{cases} \Psi_{ds} = L_{ds} i_{ds} + L_{md} i_{dr} + \Psi_m \\ \Psi_{qs} = L_{qs} i_{qs} + L_{mq} i_{qr} \end{cases} \quad (7)$$

$$\begin{cases} \Psi_{dr} = L_{dr} i_{dr} + L_{md} i_{ds} + \Psi_m \\ \Psi_{qr} = L_{qr} i_{qr} + L_{mq} i_{qs} \end{cases} \quad (8)$$

The coupling between the electrical system and the mechanical system is represented by the torque equation and the mechanical equation. The electromagnetic torque T_{el} developed by the motor can be expressed as:

$$T_{el} = \frac{p}{2} \cdot \frac{3}{2} (\Psi_{ds} i_{qs} - \Psi_{qs} i_{ds}) \quad (9)$$

The electromagnetic torque is balanced by the mechanical shaft torque T_{load} and the dynamical torque caused by the total inertia J

$$T_m = T_{load} + J \frac{d\omega_m}{dt} \quad (10)$$

B. Verification and utilization of the model

This model has been implemented in Simulink, Matlab. The maximum stator current at start can be checked and compared to the value from the induction motor. The two values have to be in the same range.

As the model is analytical, the start can be simulated in different conditions:

- The value of the inertia can be changed. With a submersible pump, having a higher inertia at start can be used to take into account the presence of water around the shaft.
- Different rotor positions can be tested as the early part of the acceleration during the start is very much dependent on the rotor position at the instant of start [4].
- The influence of a supplied-voltage drop can be analysed. It can be important to know if the motor is still able to start with a weak network.

In order to improve the starting capability of the LSPM, the main parameters that can be changed in the design are the rotor resistance, the d- and q- axis reactances X_d and X_q and the no-load voltage.

The design procedure and the dq model have been used to design a 75kW 4 pole LSPM. This power has been chosen in order to check if LSPMs could be a good solution also at that power despite a high rotor inertia.

3. Design of a 75kW, 4 poles LSPM

A. First design

The first design was completed with the following parameters: the air-gap g was chosen to be the same as for the induction motor that is $g = 1.2\text{mm}$; from a previous design, the value of the rotor resistance in per-unit was chosen equal to $R_{rpu} = 0.03\text{pu}$; the level of saturation in a tooth to $B_{tr} = 1.6\text{T}$ and the no-load voltage in per-unit to 1.

The geometry obtained is showed on figure 7. With finite elements simulations it is possible to retrieve the d- and q- reactances: $X_d = 1.68\Omega$, $X_q = 2.60\Omega$.

The steady state performances were checked, and it appeared that the maximum torque was much too low to guarantee the stability of the drive. At the same time the resistance of the rotor bar was too high to allow the motor to synchronize.

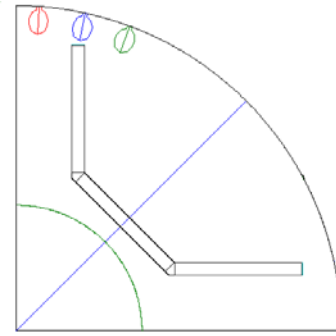


Fig. 7. Part of the rotor of the geometry 1: $g=1.2\text{mm}$; $B_{tr} = 1.6\text{T}$; $R_{rpu}=0.03$.

B. Second design

A second design was then done with a rotor bar resistance half the value of the first design. This implies that the area of a bar is larger (see figure 8) and the magnets are thicker. The level of saturation in a tooth is allowed to be higher $B_{tr} = 1.7\text{T}$, resulting in rotor bars a bit thicker.

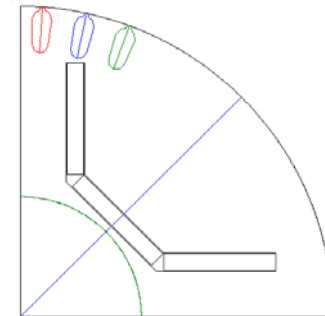


Fig. 8. Part of the rotor of the rotor of the geometry 2: $g=1.2\text{mm}$; $B_{tr} = 1.7\text{T}$; $R_{rpu}=0.15$;

With this second geometry, the values of the d- and q- axis reactances are $X_d = 1.46\Omega$, $X_q = 2.72\Omega$. The rotor resistance is low enough so that the motor synchronizes. However the maximum torque is still too low to assure

the stability (figure 9). The expression of the synchronous torque is:

$$T = \frac{3p}{2\omega_s} \left[\frac{E_0 V}{X_d} \sin \delta + \frac{V^2}{2} \left(\frac{1}{X_q} - \frac{1}{X_d} \right) \sin 2\delta \right] \quad (11)$$

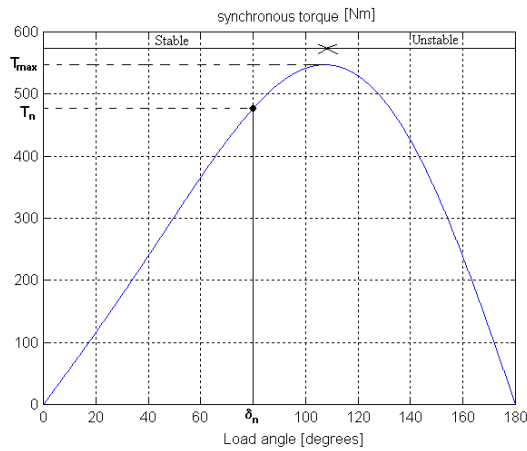


Fig. 9. Torque as a function of the load angle

By reducing the values of X_d and X_q , the maximum torque can be increased. This can be achieved by having a larger air-gap. However this requires thicker magnets and the space close to the shaft may not be sufficient. In order to have more places for the magnets, the value of the level of saturation in the rotor teeth can be chosen higher. It should be checked in the finite element simulations that this value is not exceeded.

C. Third and best design

For the third design, the value of the air-gap is chosen to $g = 1.5\text{mm}$ and $B_{tr} = 1.8\text{T}$.

Table 1 presents the geometrical and electrical parameters and the performances of the different designs.

Table I
Comparison between the three designs

	Design 1	Design 2	Design 3
Air-gap length [mm]	1.2	1.2	1.5
Saturation level in the rotor teeth [T]	1.6	1.7	1.8
Rotor cage resistance [pu]	0.03	0.015	0.015
Magnet thickness [mm]	4.6	6.3	7.7
Magnet length [mm]	136.5	125	124.7
d- axis reactance [Ω]	1.68	1.46	1.22
q- axis reactance [Ω]	2.60	2.72	2.20
Maximum torque [Nm]	494	661	836
Start?	No	Yes	Yes
Power factor	0.84	0.92	0.95
Efficiency [%]	92.9	94.0	94.5

With this third design, a good compromise has been found between the steady state and transient performances.

The start has been tested with different values of the inertia with an initial rotor position that gives the highest braking torque at initial time. Figure 10 shows that the motor can synchronize with an inertia 2.3 times higher than the rotor's own inertia.

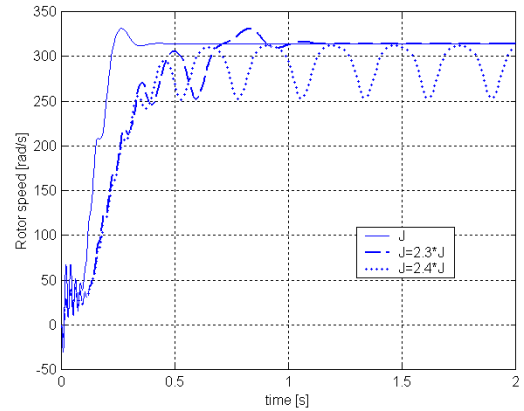


Fig. 10. Motor speed during transient start with different values of the inertia J

The capability of the LSPM to adapt to a reduced supply voltage at start has been tested (figure 11). The motor can synchronize with a supplied voltage equal to $0.85*V$ (V is the nominal phase to neutral voltage).

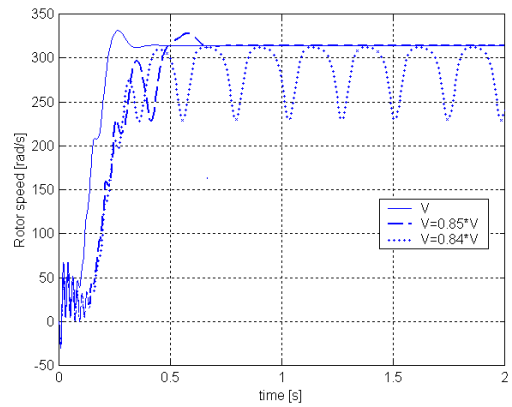


Fig. 11. Motor speed during transient start with different values of the supplied voltage V

Finally the evolution of the stator current during the transient start is presented figure 12. The current becomes between 7 and 8 times higher than the nominal current, which is in the same range as for the induction motor.

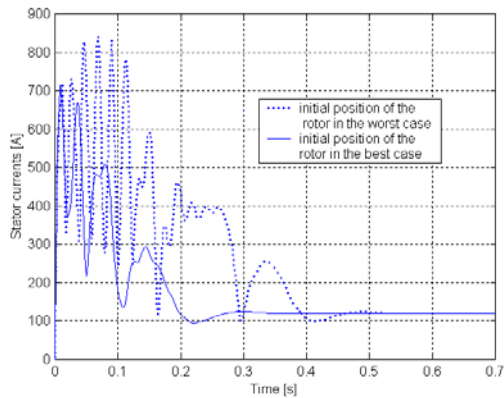


Fig. 12. Stator current during the start as a function of the time for two cases of the initial rotor position

Table II presents a comparison between the performances of the induction motor and the LSPM. The LSPM has a better efficiency as the nominal current is lower for the LSPM. The power factor is also higher for the LSPM.

Table II
Comparison between induction motor and LSPM

Parameters	Induction motor	LSPM
Efficiency	91.38	94.52
Power Factor	0.845	0.95
Nominal current [A]	140.2	119.4

4. Conclusion

A design procedure for Line Start Permanent Magnet Synchronous Motors has been presented and applied for a 75kW 4 pole submersible pump.

Different rotors geometries were tested and the performances of the motors compared, using finite element simulations to calculate the equivalent electrical parameters. The start and synchronization were carefully analysed with an analytical model because of the high inertia of this motor. A design was found giving satisfying performances during the transient start and better performances than the induction motor at steady state.

Acknowledgement

This work has been carried out at the Permanent Magnet Drive Program of the division of Electrical Machines and Power Electronics in the Royal Institute of Technology and at ITT Flygt. Flux2D, software from Cedrat has been used for the finite element simulations.

References

- [1] T.Miller, "Synchronization of Line-Start-Permanent-Magnet AC Motor", *IEEE Trans.*, vol.PAS-103, 1984, pp1822-1828.
- [2] L.Lefevre, J. Soulard, H.-P. Nee, "Design Procedure for Line-Start Permanent Magnet Motors", *Proc. IEEE Nordic*

Workshop on Power and Industrial Electronics, NORpie 2000, Aalborg, Denmark, June 2000, pp. 261-265.

[3] P. Thelin, H.-P. Nee, "Analytical Calculation of the Airgap Flux Density of PM Motors with Buried Magnets", *Proc. ICEM 98, Istanbul, Turkey, 1998, vol. 2, pp 1166-1171.*

[4] J. Soulard, H.-P. Nee, "Study of the Synchronization of Line-Start Permanent Magnet Synchronous Motors", *Proc. IEEE Industry Applications Society Annual Meeting, Roma, Italy, 2000, pp. 424-431 vol1.*

[5] P. Thelin, J. Soulard, H.-P. Nee, and C. Sadarangani: "Comparison between Different Ways to Calculate the Induced No-Load Voltage of PM Synchronous Motors using Finite Element Methods", *Proc. 4th IEEE International Conference on Power Electronics and Drive Systems, PEDS'01, Bali, Indonesia, October 2001, pp. 468-474.*

[6] L. Lefevre, J. Soulard, "Finite Element Transient Start of a Line-Start Permanent Magnet Synchronous Motor", *Proc. ICEM 2000, Helsinki, Finland, pp. 1564-1568, vol3.*

[7] A. Knight, C. McClay, "The Design of High Efficiency Line-Start Motors", *IEEE IAS Trans.*, 2000 vol. 36, no5, pp. 1555-1562.